Pressure dependence of the magnetic anisotropy in the single-molecule magnet $Mn_4O_3Br(OAc)_3(dbm)_3$

Andreas Sieber, Grégory Chaboussant, Roland Bircher, Colette Boskovic, and Hans U. Güdel
Department of Chemistry and Biochemistry, University of Bern, Freiestrasse 3, CH-3000 Bern 9, Switzerland

George Christou
Department of Chemistry, University of Florida, Gainesville, Florida 32611, USA

Hannu Mutka
Institut Laue-Langevin, 6 rue Jules Horowitz, BP 156, 38042 Grenoble Cedex 9, France
(Received 9 September 2004; published 23 November 2004)

The anisotropy splitting in the ground state of the single-molecule magnet $Mn_4O_3Br(OAc)_3(dbm)_3$ is studied by inelastic neutron scattering as a function of hydrostatic pressure. This allows a tuning of the anisotropy and thus the energy barrier for slow magnetization relaxation at low temperatures. The value of the negative axial anisotropy parameter D_{cluster} changes from $-0.0627(1)$ meV at ambient to $-0.0603(3)$ meV at 12 kbar pressure, and in the same pressure range the height of the energy barrier between up and down spins is reduced from 1.260(5) meV to 1.213(9) meV. Since the Mn—Br bond is significantly softer and thus more compressible than the Mn—O bonds, pressure induces a tilt of the single ion Mn^{3+} anisotropy axes, resulting in the net reduction of the axial cluster anisotropy.

DOI: 10.1103/PhysRevB.70.172413 PACS number(s): 75.50.Xx, 75.30.Gw, 75.45.+j, 78.70.Nx

Single-molecule magnets (SMM) are presently the focus of a very intense research activity. SMM are molecules containing a finite number of exchange coupled magnetic ions, so-called spin clusters, which exhibit phenomena such as slow relaxation and quantum tunneling of the magnetization at low temperatures.[1] They are the smallest known units that are potentially capable of storing a bit of information at cryogenic temperatures. An easy axis type magnetic anisotropy is an essential prerequisite for an energy barrier between up and down spins and thus for slow relaxation. The height of this barrier is determined by both the ground state S value and the size of the negative D_{cluster} value in the axial spin Hamiltonian

$$\hat{H}_{\text{axial}} = D_{\text{cluster}}\left(\hat{S}_z^2 - \frac{1}{3}S(S+1)\right). \tag{1}$$

For even and odd S values the barrier height is given by $|D_{\text{cluster}}|S^2$ and $|D_{\text{cluster}}|\left(S^2-\frac{1}{4}\right)$, respectively. Chemists have been able to assemble numerous spin clusters which show SMM features at the very lowest temperatures but the number of examples with blocking temperatures above 1 K is still rather limited. Among them is a family of tetranuclear manganese clusters with general formula $Mn_4O_3X(OAc)_3(dbm)_3$, where OAc^- is the acetate ion and dbm^- is the anion of dibenzoylmethane. They all exhibit SMM behavior with an energy barrier of the order of 1.25 meV.[2] We report the first direct spectroscopic determination of the anisotropy splitting in a SMM under hydrostatic pressure. The molecule $Mn_4O_3Br(OAc)_3(dbm)_3$ (Mn_4) belongs to the above family, and its molecular structure is shown in Fig. 1(a).

The molecule has a $Mn^{4+}(Mn^{3+})_3(\mu_3-O)_3(\mu_3-Br)^{6+}$ core with a distorted cubane geometry, which is schematically depicted in Fig. 1. The molecular point symmetry is approximately C_{3v} with the C_3 axis passing through the Mn^{4+} and Br^- ions [Fig. 1(b)].[3] We correlate the pressure dependence of the anisotropy splitting with pressure induced changes in the structure and identify the dominant terms and factors which govern the anisotropy splitting and thus the barrier height.

Inelastic neutron scattering (INS) is the most direct technique to measure anisotropy splittings in SMMs in the absence of an external magnetic field. Among others, anisotropy parameters have thus been obtained for the prototype SMMs Mn_{12}-acetate[4] and $Fe_8O_2(OH)_{12}(tacn)_6^{8+}$ (Ref. 5) as well as four members of the Mn_4 cubane family including the title compound.[2]

The present measurements were carried out on a partially deuterated (acetate 99%) sample with composition $Mn_4O_3Br(d_3\text{-}OAc)_3(dbm)_3$ using the time-of-flight spectrometer IN5 at the Institut Laue Langevin (ILL) in Grenoble. The sample was prepared according to Ref. 6. For pressures of 0, 3, and 5 kbar about 2 g of polycrystalline sample placed in a standard ILL continuously loaded high-pressure cell with He as the pressure transmitting medium were used. For 12 kbar the standard ILL high-pressure clamped cell was employed with about 0.3 g of sample. Neutron wavelengths of 7.5 Å (0 to 12 kbar) and 8.5 Å (0 to 5 kbar) were used, corresponding to instrumental resolutions of 32 and 19 μeV, respectively. The data treatment involved the calibration of the detectors by means of a spectrum of vanadium metal.

Experimental results for 0, 5, and 12 kbar at 18 K are shown in Fig. 2(a). At this temperature all the ground state levels have some population. At all pressures four well resolved inelastic peaks, labeled I–IV, are observed on both the energy loss and gain side, corresponding to positive and

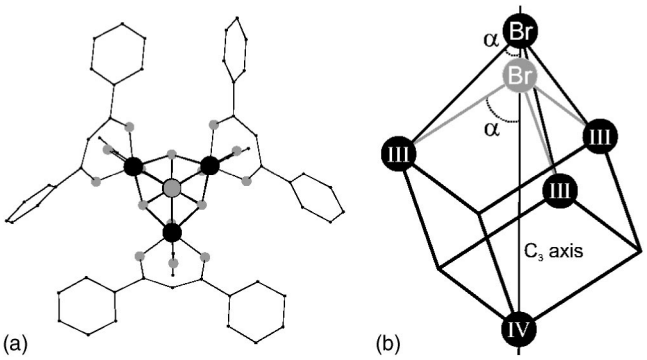

FIG. 1. (a) Molecular structure of the title complex Mn_4, from Ref. 3. View along the approximate C_3 axis. For clarity the H atoms are omitted. Mn^{3+} ions are drawn as large black spheres, C and O atoms as small black and grey spheres, respectively. The large grey sphere represents the Br^- ion, which obscures the Mn^{4+} ion just behind; (b) schematic view of the core of Mn_4, with III and IV representing Mn^{3+} and Mn^{4+}, respectively. The black and grey positions of the Br^- ion schematically represent the situation at ambient and high external pressure, respectively.

negative energy transfers in Fig. 2(a), respectively. The 12 kbar peaks are slightly inhomogeneously broadened. At 2 K only peak I is observed, and this is shown on an expanded energy scale in Fig. 2(b). A decrease of the peak energy with pressure is evident. An analysis using Gaussian fits to the background corrected data yields the peak positions in Table I. The data at ambient pressure are in good agreement with those reported in Ref. 2.

Antiferromagnetic exchange interactions between the three Mn^{3+} ($S=2$) ions and the Mn^{4+} $\left(S=\frac{3}{2}\right)$ ion dominate the coupling in Mn_4, thus leading to a $S=\frac{9}{2}$ cluster ground state, with the first excited $S=\frac{7}{2}$ state at about 22 meV and thus outside the range of our experiment. The trigonal symmetry of the Mn_4 molecules in the crystal structure of the title compound is slightly distorted, as can be seen in Fig. 1(a), with an actual point group symmetry C_1. Including a higher order term the appropriate spin Hamiltonian to account for the splitting of the $S=\frac{9}{2}$ ground state is thus given by

$$\hat{H}_{\mathrm{ani}} = D_{\mathrm{cluster}}\left[\hat{S}_z^2 - \frac{1}{3}S(S+1)\right] + B_4^0\hat{O}_4^0 + E(\hat{S}_x^2 - \hat{S}_y^2), \quad (2)$$

where $\hat{O}_4^0 = 35\hat{S}_z^4 - [30S(S+1)-25]\hat{S}_z^2 - 6S(S+1) + 3\hat{S}^2(S+1)^2$.

From the data in Ref. 2 the following parameter values at 18 K were determined: $D_{\mathrm{cluster}} = -0.062$ meV, $B_4^0 = -6.3 \times 10^{-6}$ meV and $|E| = 2.1 \times 10^{-3}$ meV. The first term in Eq. (2) is the leading term, and thus M_S remains a reasonably good quantum number. The splitting pattern with the above parameters is shown in Fig. 3. Magnetic neutron scattering theory leads to the selection rules $\Delta M_S = 0, \pm 1$ for INS, i.e., transitions between adjacent levels are allowed, see the arrows in Fig. 3. We can thus immediately assign the observed INS bands I–IV in Fig. 2 as given in the second column of Table I. Fitting the eigenvalues of Eq. (2) to the observed band energies yields the parameter values at the bottom of Table I. Both $|B_4^0|$ and $|E|$ are much smaller than $|D_{\mathrm{cluster}}|$, but they are essential for a proper description, and they are responsible for the deviations from a regular spacing of the peaks in Fig. 2(a). The parameter values at ambient pressure are the same within experimental accuracy as those derived from the data in Ref. 2. The negative D_{cluster} is significantly pressure dependent, its value decreasing linearly by 3.8% between ambient pressure and 12 kbar. This leads to a reduction of the energy barrier, i.e., the energy difference between the $M_S = \pm\frac{1}{2}$ and $M_S = \pm\frac{9}{2}$ levels, from 1.260(5) meV at ambient to 1.213(9) meV at 12 kbar pressure, respectively. The pressure dependence of B_4^0 and E is too small to be determined by our experiment.

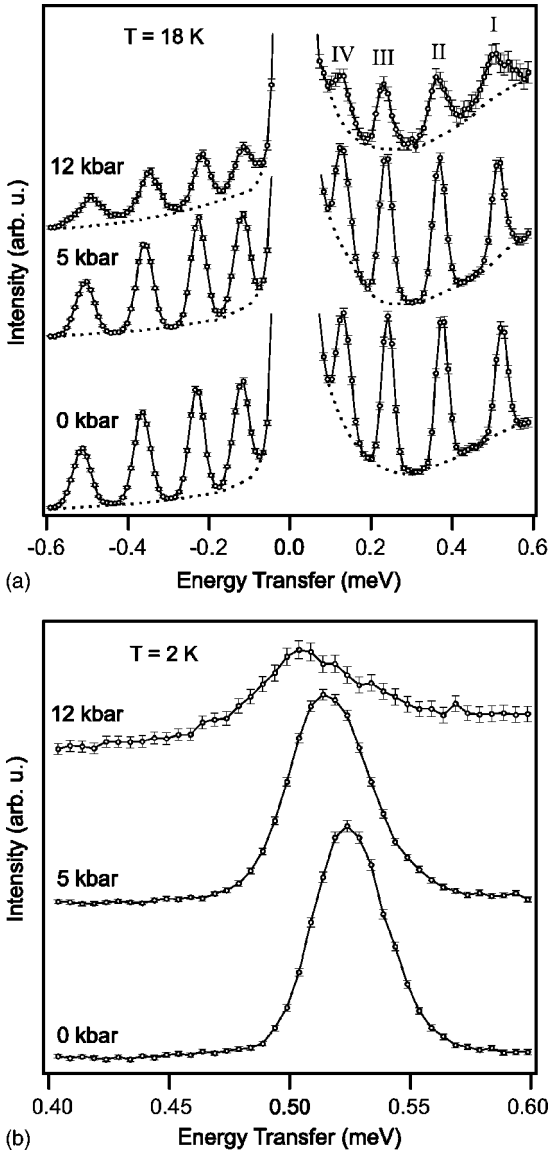

FIG. 2. (a) INS spectra at 18 K of a polycrystalline sample of partially deuterated $Mn_4O_3Br(d_3\text{-}OAc)_3(dbm)_3$ recorded on IN5 with an incident wavelength $\lambda_i = 7.5$ Å for pressures $p = 0$, 5, and 12 kbar. The spectra correspond to the sum of all the scattering angles. The labeling of the peaks corresponds to Table I and Fig. 3. The full lines connect adjacent data points. The dotted lines illustrate the background which was approximated by polynomials and subtracted from the data; (b) pressure dependence of peak I at 2 K.

The only pressure experiments on single-molecule mag-

TABLE I. Experimental INS peak positions and calculated transition energies using Eq. (2) as a function of hydrostatic pressure. The labeling corresponds to Fig. 2, and the assignments in the second column refer to Fig. 3. Parameter values for each pressure are given at the bottom. The pressure dependence of $|E|$ and B_4^0 is too small to be determined in this experiment, and the values determined at ambient pressure were used throughout.

		Energy (meV)							
		$p=0$ kbar		$p=3$ kbar		$p=5$ kbar		$p=12$kbar	
Label	Transition	exp.	calc.	exp.	calc.	exp.	calc.	exp.	calc.
I	$\pm 9/2 \leftrightarrow \pm 7/2$	0.522(1)	0.522	0.517(1)	0.517	0.514(1)	0.514	0.503(1)	0.503
II	$\pm 7/2 \leftrightarrow \pm 5/2$	0.373(1)	0.373	0.369(1)	0.369	0.366(1)	0.367	0.359(3)	0.359
III	$\pm 5/2 \leftrightarrow \pm 3/2$	0.238(1)	0.238	0.235(1)	0.235	0.233(1)	0.233	0.227(2)	0.228
IV	$\pm 3/2 \leftrightarrow \pm 1/2$	0.127(2)	0.127	0.126(1)	0.126	0.125(1)	0.125	0.124(3)	0.123
	D_{cluster}	$-0.0627(1)$		$-0.0620(1)$		$-0.0616(1)$		$-0.0603(3)$	
	$\lvert E\rvert$	$1.90(1)\times 10^{-3}$		1.90×10^{-3}		1.90×10^{-3}		1.90×10^{-3}	
	B_4^0	$-6.2(2)\times 10^{-6}$		-6.2×10^{-6}		-6.2×10^{-6}		-6.2×10^{-6}	

nets reported in the literature are for Mn_{12}-acetate. From the pressure dependence of the low temperature magnetization it was concluded that pressure produces a geometrical molecular isomer of Mn_{12}-acetate with significantly faster relaxation of the magnetization.[7] On the other hand, changes in the position of the steps in the hysteresis of Mn_{12}-acetate under pressure were ascribed to an increase of the axial anisotropy splitting with pressure.[8] Our experimental finding for Mn_4 that the axial anisotropy splitting is decreasing with pressure is unambiguous. With the following simplified model we account for this decrease by correlating it with the expected structural changes of the molecule under pressure. We assume an isotropic compressibility for the core defined by the three Mn^{3+} ions and the Mn^{4+} ion in Fig. 1(b). All the metal-ligand bonds in this core are either $Mn^{3+}-O$ or $Mn^{4+}-O$ bonds, and taking average linear compressibilities (d) from the literature we calculate $d(12\text{ kbar})/d(\text{ambient})=0.9975$.[9] The $Mn^{3+}-Br$ bonds in Fig. 1 are significantly softer and more compressible than the Mn–O bonds. A ratio of force constants $k(Mn^{3+}-O)/k(Mn^{3+}-Br)=4.2$ is obtained from literature values based on Raman experiments.[10,11] In terms of compressibility we thus calculate a ratio $d(12\text{ kbar})/d(\text{ambient})=0.993$ for the $Mn^{3+}-Br$ bonds. The net effect of pressure in this simplified model is an increase of the apex angle at the Br position of the molecule. Between ambient and 12 kbar pressure this angle α, defined in Fig. 1(b), increases from 42.5° to 42.75°. Since the Jahn-Teller axis of the Mn^{3+} coordination is close to the Mn–Br direction, pressure induces an inward tilt of the three Mn^{3+} anisotropy axes, thus decreasing the cluster anisotropy. The value of the axial anisotropy parameter of the cluster in the $S=\frac{9}{2}$ ground state can be expressed as:[12]

$$D_{\text{cluster}} = \frac{105}{484} D_{\text{Mn}^{3+}} (3\cos^2\alpha - 1) + \frac{35}{121} D_{33} - \frac{7}{44} D_{34}, \tag{3}$$

where $D_{\text{Mn}^{3+}}$ is the single ion D parameter of the Mn^{3+}, D_{33} and D_{34} are magnetic dipole–dipole interaction terms between $Mn^{3+}-Mn^{3+}$ and $Mn^{3+}-Mn^{4+}$, respectively. These latter two terms in Eq. (3) can be calculated,[12] they are typically an order of magnitude smaller than the experimental $|D_{\text{cluster}}|$, and their sum is practically pressure independent, see Table II. We can thus definitely rule out that the observed reduction of $|D_{\text{cluster}}|$ with pressure is due to a change in the dipole–dipole interaction. On the other hand, the $(3\cos^2\alpha - 1)$ factor in the first term of Eq. (3) has a significant effect. With the estimated increase of α by 0.25° at 12 kbar we calculate a 2.1% reduction of the $|D_{\text{cluster}}|$ value at 12 kbar. This is to be compared with the reduction of 3.8% derived experimentally. We note that for $\alpha=42.5°$ in Mn_4 the function $(3\cos^2\alpha - 1)$ is highly susceptible to minute changes of α. Since our compressibility model is rather crude, the estimated pressure dependence of α has a relatively large uncertainty, which is amplified for the factor $(3\cos^2\alpha - 1)$. In this rough estimate we have neglected any pressure dependence of $D_{\text{Mn}^{3+}}$ in Eq. (3). According to Ref. 13 $|D_{\text{Mn}^{3+}}|$ can either increase or decrease with increasing crystal field strength,

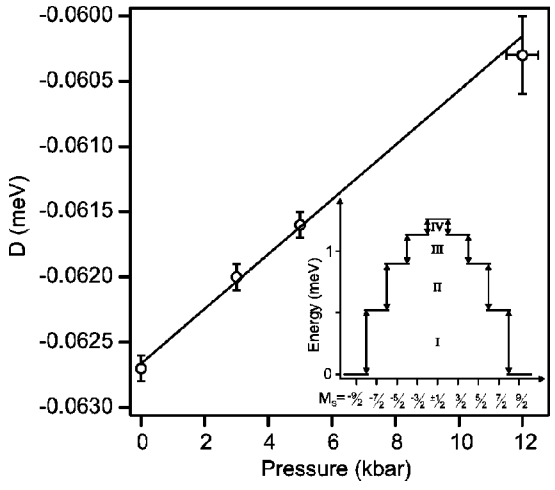

FIG. 3. Experimental variation of D_{cluster} as a function of pressure with a linear least-squares fit. The inset shows the calculated ansisotropy splitting in the $S=\frac{9}{2}$ ground state using the parameter values at ambient pressure in Table I. The double arrows correspond to the allowed $\Delta M_S=\pm 1$ INS transitions.

TABLE II. D_{cluster} values of $Mn_4O_3X(OAc)_3(dbm)_3$ (X=Cl, Br) determined by INS. D_{dd} is the calculated sum of the two dipole–dipole contributions D_{33} and D_{34} in Eq. (3). $D_{Mn^{3+}}$ is the single-ion D parameter calculated from D_{cluster} using Eq. (3). α is the angle at the apex of the cluster defined in Fig. 1(b), and $(3\cos^2\alpha-1)$ is the factor in the first term of Eq. (3).

X=	D_{cluster} (meV) observed	D_{dd} (meV) calculated[b]	$D_{Mn^{3+}}$ (meV) calculated	α (°)	$(3\cos^2\alpha-1)$
Br, ambient	−0.0627(1)	0.0082	−0.52	42.5(2)[c]	0.63
Br, 12 kbar	−0.0603(3)	0.0083	−0.52[d]	42.75[e]	0.62
Cl[a]	−0.0656	0.0085	−0.68	45.1(1)[c]	0.50

[a]Reference 2.
[b]Calculated using Ref. 12.
[c]Reference 3.
[d]Assumed to be pressure independent.
[e]Calculated as described.

depending on its absolute value. In Mn_{12}-acetate, where the Mn^{3+} coordination is very similar to the title compound, a small increase of $|D_{Mn^{3+}}|$ with pressure is deduced from magnetization experiments.[8] Our assumption that the decrease of $|D_{\text{cluster}}|$ with pressure in our Mn_4 cluster is not due to a decrease of $|D_{Mn^{3+}}|$ is thus justified. Despite the approximate character of our model, we therefore feel confident that we have identified the principal structural element in Mn_4, which leads to a decrease of the axial anisotropy under hydrostatic pressure. The compression of the apex with the resulting increase of α is schematically represented in Fig. 1(b) by the grey Br position.

Chemical variation is another way of tuning the cluster anisotropy. In Table II we compare the effect of hydrostatic pressure on the Mn_4Br compound with a chemical substitution of Br by Cl at ambient pressure. While physical pressure mainly affects the $(3\cos^2\alpha-1)$ factor in the first term of Eq. (3), substitution of Br by Cl strongly increases the value of the negative single-ion anisotropy parameter $D_{Mn^{3+}}$ and thus more than compensates for the decrease of the $(3\cos^2\alpha-1)$ factor. The result of the chemical substitution from Br to Cl is thus an increase of $|D_{\text{cluster}}|$, while hydrostatic pressure of 12 kbar reduces it by about the same amount.

In conclusion, we have presented the first direct determination of the pressure dependence of the axial anisotropy splitting in a SMM. Hydrostatic pressure of 12 kbar reduces the energy barrier between plus and minus spins by 3.8%. The reduction mainly results from a tilting of the single ion anisotropy axes of Mn^{3+} under pressure. Very recent INS experiments confirm that in the SMM Mn_{12}-acetate $|D_{\text{cluster}}|$ slightly increases with pressure.[8] This different behavior confirms our conclusion that the pressure dependence is a property determined by the specific structure of a SMM molecule.

ACKNOWLEDGMENTS

The authors thank Oliver Waldmann and Graham Carver for fruitful discussions. This work was financially supported by the Swiss National Science Foundation (NFP 47) and the European Union (TMR Molnanomag, No. HPRN-CT-1999-00012).

[1] D. Gatteschi and R. Sessoli, Angew. Chem., Int. Ed. **42**, 268 (2003).
[2] H. Andres, R. Basler, H. U. Güdel, G. Aromi, G. Christou, H. Büttner, and B. Ruffle, J. Am. Chem. Soc. **122**, 12469 (2000).
[3] S. Wang, H.-L. Tsai, E. Libby, K. Folting, W. E. Streib, D. N. Hendrickson, and G. Christou, Inorg. Chem. **35**, 7578 (1996).
[4] I. Mirebeau, M. Hennion, H. Casalta, H. Andres, H. U. Güdel, A. V. Irodova, and A. Caneschi, Phys. Rev. Lett. **83**, 628 (1999).
[5] R. Caciuffo, G. Amoretti, A. Murani, R. Sessoli, A. Caneschi, and D. Gatteschi, Phys. Rev. Lett. **81**, 4744 (1998).
[6] G. Aromi, S. Bhaduri, P. Artus, K. Folting, and G. Christou, Inorg. Chem. **41**, 805 (2002).
[7] Y. Suzuki, K. Takeda, and K. Awaga, Phys. Rev. B **67**, 132402 (2003).
[8] Y. Murata, K. Takeda, T. Sekine, M. Ogata, and K. Awaga, J. Phys. Soc. Jpn. **67**, 3014 (1998).
[9] R. M. Hazen and L. W. Finger, *Comparative Crystal Chemistry* (Wiley, New York, 1982), p. 152.
[10] A. Cua, J. S. Vrettos, J. C. de Paula, G. W. Brudvig, and D. F. Bocian, JBIC, J. Biol. Inorg. Chem. **8**, 439 (2003).
[11] K. Nakamoto, *Infrared and Raman Spectra of Inorganic and Coordination Compounds* (Wiley, New York, 1997), Part A, pp. 216–217.
[12] A. Bencini and D. Gatteschi, *EPR of Exchange Coupled Systems* (Springer, New York, 1989), pp. 68–70 and pp. 100–106.
[13] A. Bencini, I. Ciofini, and M. G. Uytterhoeven, Inorg. Chim. Acta **274**, 90 (1998).